Optica Imaging Congress © 2024 Optica Publishing Group

High-resolution Space-variant Shack–Hartmann Wavefront Reconstruction

Fan Feng,[1,*] Chen Liang,[2]

[1] *GBA Institute of Collaborative Innovation, Guangzhou 510300, China*
[2] *LMAM, School of Mathematical Sciences, Peking University, Beijing 100871, China*

[*] *ffeng@pku.edu.cn*

Abstract: Space-variant wavefront reconstruction plays a crucial role in large field-of-view imaging. Instead of using affine transformation, displacement fields of subimages within Shack–Hartmann sensor are evaluated using polynomial model, resulting in improved resolution for space-variant functions.

1. Introduction

Achieving expansive field-of-view (FOV) imaging in both astronomy and microscopy presents challenges due to atmospheric turbulence and the heterogeneous properties of biological tissues. Researchers have developed various adaptive optics (AO) systems tailored to specific scientific goals to overcome these obstacles in astronomy, such as Multi-Conjugate Adaptive Optics (MCAO) [1], Multi-Object Adaptive Optics (MOAO) [2], Ground Layer Adaptive Optics (GLAO) [3]. While these AO systems excel in astronomy, their high complexity and costs may render them unsuitable for microscopy applications, especially considering photon loss. In microscopy, simpler methods are preferred. For instance, the homogeneous area method, adopted in various microscopes [4], reconstructs and corrects wavefronts from segmented zones within a small FOV. However, this approach involves multiple acquisitions, leading to a trade-off between spatial resolution and acquisition speed.

The Shack-Hartmann sensors capture subimage deformations rather than simple translational shifts when space-variant wavefronts exist. Our prior publications [5,6] propose innovative methods for sensing space-variant wavefronts using the Shack-Hartmann sensor. These approaches involve characterizing the space-variant function through either six coefficients associated with affine transformations or five coefficients excluding shear transformations.

In our current work, we adopt a polynomial model to provide greater flexibility in characterizing space-variant functions, resulting in higher resolution.

2. Method

The affine transformation with six coefficients was previously used to characterize the deformation of a pair of subimages [5]

$$\begin{aligned}\Delta x &= a_0 + a_{10}x_1 + a_{01}y_1 \\ \Delta y &= b_0 + b_{10}x_1 + b_{01}y_1\end{aligned} \tag{1}$$

Apparently, Eq.(1), intuitively and inevitably, could be generalized to the polynomial transformation

$$\begin{aligned}\Delta x &= a_0 + a_{10}x_1 + a_{01}y_1 + a_{20}x_1^2 + a_{11}x_1y_1 + a_{02}y_1^2 + a_{30}x_1^3 + \cdots \\ \Delta y &= b_0 + b_{10}x_1 + b_{01}y_1 + b_{20}x_1^2 + b_{11}x_1y_1 + b_{02}y_1^2 + b_{30}x_1^3 + \cdots\end{aligned} . \tag{2}$$

Various registration algorithms could be used to obtain high resolution displacement fields, such as iterative optimization based on image similarity, optical flow, piecewise rigidity correlation [7], diffeomorphic demons [8] and free form deformation [9]. After that, the space-variant wavefront function could be reconstructed by the same framework in Ref. [5,6].

3. Results and Conclusions

In our simulations, we adopt a configuration and parameters similar to those in Ref. [5]. Specifically, we consider a simulated template phase screen denoted as P, with dimensions of 1185×1185 pixels. This phase screen exhibits a smooth distribution with a peak-to-valley (PV) value of 14.124 radians and a root mean square (RMS) value of 2.80 radians. The space-variant wavefront, represented by W, consists of $37 \times 37 \times 465 \times 465$ pixels while the Fourier domain occupies 465×465 pixels and the space domain spans 37×37 pixels. We set that the space-variant wavefront adjected in 1 pixel in the space domain corresponds to a 20 pixels in the Fourier domain. For instance:

$W(1,1,465,465) = P(1:465,1:465), W(1,2,465,465) = P(1:465,21:485)$. To estimate the displacement field, we employ a free-form deformation registration algorithm. Subsequently, we fit 5th-order polynomial functions to the resulting data. Figure 1 illustrates that the free-form algorithm yields higher resolution in the space domain, with an average RMS nearly one-third smaller than that obtained using the affine algorithm.

In this study, we introduced a high-resolution method for reconstructing space-variant wavefronts using Shack–Hartmann sensors. Leveraging free-form registration and a polynomial model, we enhance the characterization of fine structures within the space-variant function. Our reconstruction results demonstrate an average root mean square reduction of one-third compared to the results obtained using the affine algorithm.

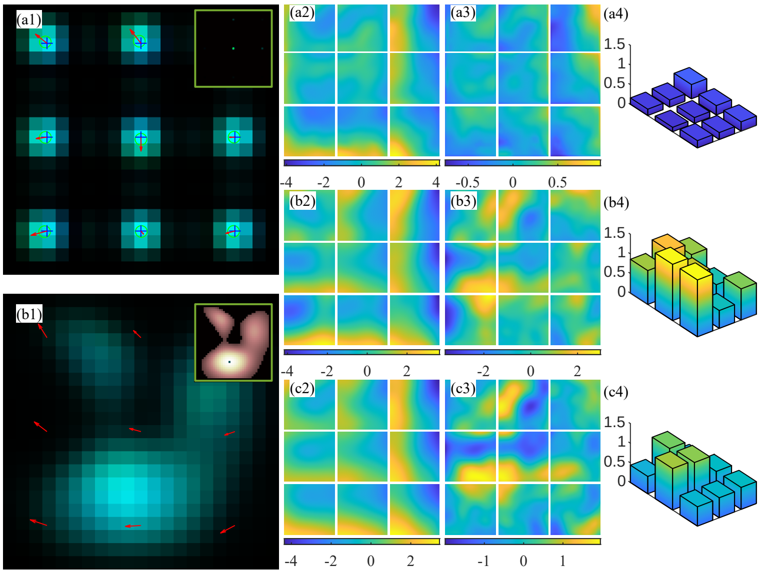

Fig. 1. Comparisons of wavefront reconstruction results. The SH subimage without (blue) and with (green) perturbation, illuminated by (a1) 3 × 3 star array and (b1) peaks pattern. light source presented on the up-right corner. (a2-c2) Reconstruction wavefronts by using (a2) Centroid algorithm with 3 × 3 stars illuminated, (b2) affine estimation, (c2) free form deformation. Residual wavefronts (a3-c3) between (a2-c2) and ground truth. (a4-c4) RMS of the corresponding residual wavefronts.

References

1. J. M. Beckers, Increasing the size of the isoplanatic patch with multiconjugate adaptive optics, 1988.
2. M. Lamb, K. Venn, D. Andersen, S. Oya, M. Shetrone, A. Fattahi, L. Howes, M. Asplund, O. Lardière, M. Akiyama, Y. Ono, H. Terada, Y. Hayano, G. Suzuki, C. Blain, K. Jackson, C. Correia, K. Youakim, C. Bradley, Using the multi-object adaptive optics demonstrator raven to observe metal-poor stars in and towards the galactic centre, Monthly Notices of the Royal Astronomical Society 465 (3) (2016) 3536–3557.
3. F. Rigaut, Ground conjugate wide field adaptive optics for the elts (2002).
4. T.-L. Liu, S. Upadhyayula, D. E. Milkie, V. Singh, K. Wang, I. A. Swinburne, K. R. Mosaliganti, Z. M. Collins, T. W. Hiscock, J. Shea, A. Q. Kohrman, T. N. Medwig, D. Dambournet, R. Forster, B. Cunniff, Y. Ruan, H. Yashiro, S. Scholpp, E. M. Meyerowitz, D. Hockemeyer, D. G. Drubin, B. L. Martin, D. Q. Matus, M. Koyama, S. G. Megason, T. Kirchhausen, E. Betzig, Observing the cell in its native state: Imaging subcellular dynamics in multicellular organisms, Science 360 (6386) (2018) eaaq1392.
5. F. Feng, C. Liang, D. Chen, K. Du, R. Yang, C. Lu, S. Chen, L. Chen, L. Tao, H. Mao, Space-variant shack-hartmann wavefront sensing based on affine transformation estimation, Applied Optics 61 (32) (2022) 9342–9349.
6. F. Feng, C. Liang, D. Chen, K. Du, R. Yang, C. Lu, S. Chen, W. He, P. Xu, L. Chen, L. Tao, H. Mao, Moment-based space-variant shack–hartmann wavefront reconstruction, Optics Communications 540 (2023) 129515.
7. J. Wu, Z. Lu, D. Jiang, Y. Guo, H. Qiao, Y. Zhang, T. Zhu, Y. Cai, X. Zhang, K. Zhanghao, H. Xie, T. Yan, G. Zhang, X. Li, Z. Jiang, X. Lin, L. Fang, B. Zhou, P. Xi, J. Fan, L. Yu, Q. Dai, Iterative tomography with digital adaptive optics permits hour-long intravital observation of 3d subcellular dynamics at millisecond scale, Cell 184 (12) (2021) 3318–3332.e17.
8. T. Vercauteren, X. Pennec, A. Perchant, N. Ayache, Diffeomorphic demons: Efficient non-parametric image registration, Neuroimage 45 (1) (2009) S61–S72.
9. Z. Y. Xie, G. E. Farin, Image registration using hierarchical b-splines, IEEE Transactions on Visualization and Computer Graphics 10 (1) (2004) 85–94, xie, ZY Farin, GE.